Green extraction of polyphenolic lignin using FeCl3-mediated tartaric acid-DES and its derived lignin nanoparticles for enhancing the application performance of PVA film in green agriculture

Yadan Luo [a], Linlin Liang [a,b], Huaying Luo [c], Fanyan Zeng [a], Chengrong Qin [a], Chen Liang [a], Baojie Liu [a], Caoxing Huang [b], Shuangquan Yao [a]**

[a] Guangxi Key Laboratory of Clean Pulp & Papermaking and Pollution Control, School of Light Industry and Food Engineering, Guangxi University, Nanning, 530004, PR China

[b] Jiangsu Co-Innovation Center of Efficient Processing and Utilization of Forest Resources, Nanjing Forestry University, Nanjing 210037, PR China

[c] Xianhe Co,.Ltd, Quzhou, 324022, PR China

[*]Corresponding author: yaoshuangquan@gxu.edu.cn (Shuangquan Yao)

qinchengrong@gxu.edu.cn (Chengrong Qin)

1. Experimental section

1.1 Compositional analysis of remaining solids

The separation yields of cellulose, hemicellulose, and lignin were determined according to the NREL method published by the U.S. Department of Energy. Glucose and xylose in the acid hydrolysate were determined using gel permeation chromatography, and acid-soluble lignin was detected using an UV spectrophotometer at 205 nm. The residue after filtration of the acid hydrolysate is washed to neutrality with deionized water and dried at 105°C. The mass of the residue weighed by the difference method is the mass of the acid-insoluble lignin. Finally, the separation yields of cellulose, hemicellulose, and lignin were calculated using the following formula:

$$R_C = (C_1 - C_2)/C_1 \times 100 \quad \text{(Eq. 1)}$$

$$R_H = (C_3 - C_4)/C_3 \times 100 \quad \text{(Eq. 2)}$$

$$R_L = (C_5 - C_6)/C_5 \times 100 \quad \text{(Eq. 3)}$$

where R_C represents the cellulose separation yield (%), C_1 represents the cellulose content of the raw material (%), C_2 represents the cellulose content of the remaining solid (%), R_H represents the hemicellulose separation yield (%), C_3 is the hemicellulose content (%), C_4 represents the remaining solid hemicellulose content (%), R_L represents the lignin separation yield (%), C_5 represents the lignin content of the raw material (%), and C_6 represents the lignin content of the remaining solid (%).

1.2 Physicochemical properties of remaining solids

The morphology of the raw materials and the residual solids after treatment with

different DES systems was observed using a Scanning Electron Microscope (SU8020, Hitachi, Tokyo, Japan). Lignin in plant cell walls can be visually observed using a Confocal Laser Scanning Microscope (Leica TCS SP8, Leica, Wetzlar, Germany) because lignin can be excited to fluoresce. The changes of the main functional groups of the substrates after treatment were analyzed using Fourier transform infrared spectroscopy (IRTracer-100, Shimadzu, Kyoto, Japan), X-ray diffractometer (ESCALAB 250XI, Thermo, Massachusetts, USA) and (CP/MAS) ^{13}C NMR (VNMRS 600, Agilent, California, USA). The thermal stability and crystallinity of the treated substrates were characterized by TGA (STA 449F5, Netzsch, Bavaria, Germany) and XRD (D/MAX2500V, Rigaku, Tokyo, Japan).

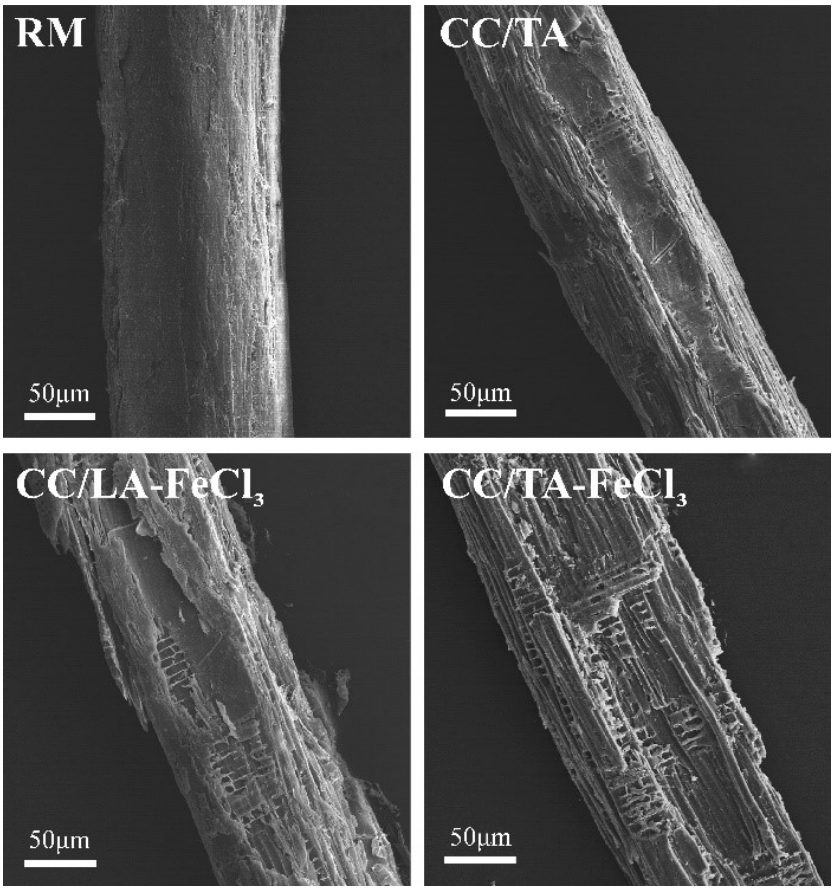

Fig. S1. SEM analysis of eucalyptus substrate before and after different DES treatment

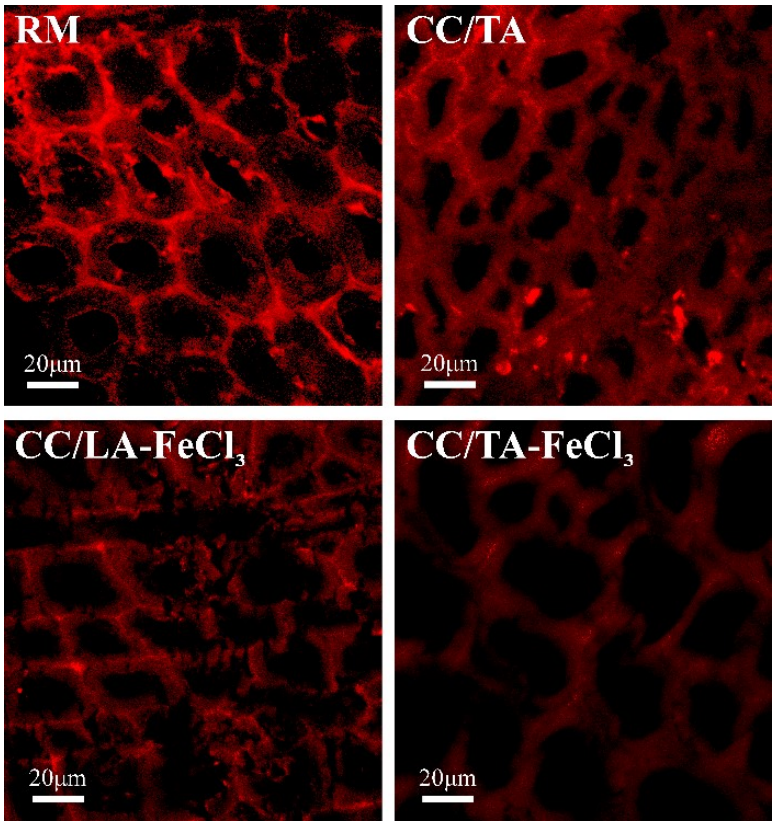

Fig. S2. CLSM analysis of eucalyptus substrate before and after different DES treatment

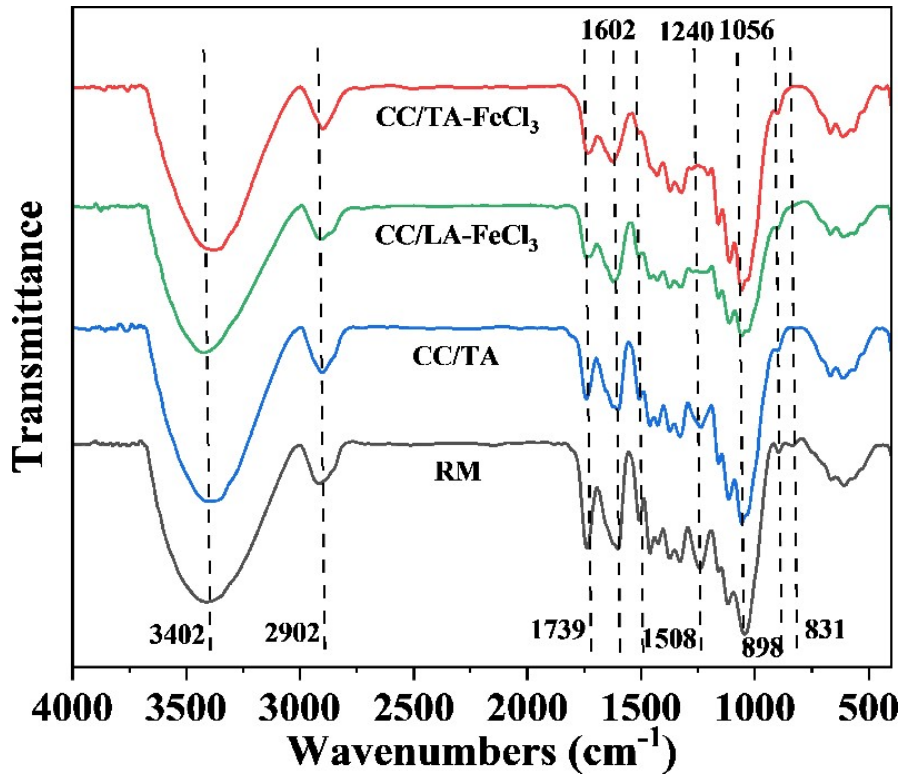

Fig. S3. FT-IR analysis of eucalyptus substrate before and after different DES treatment

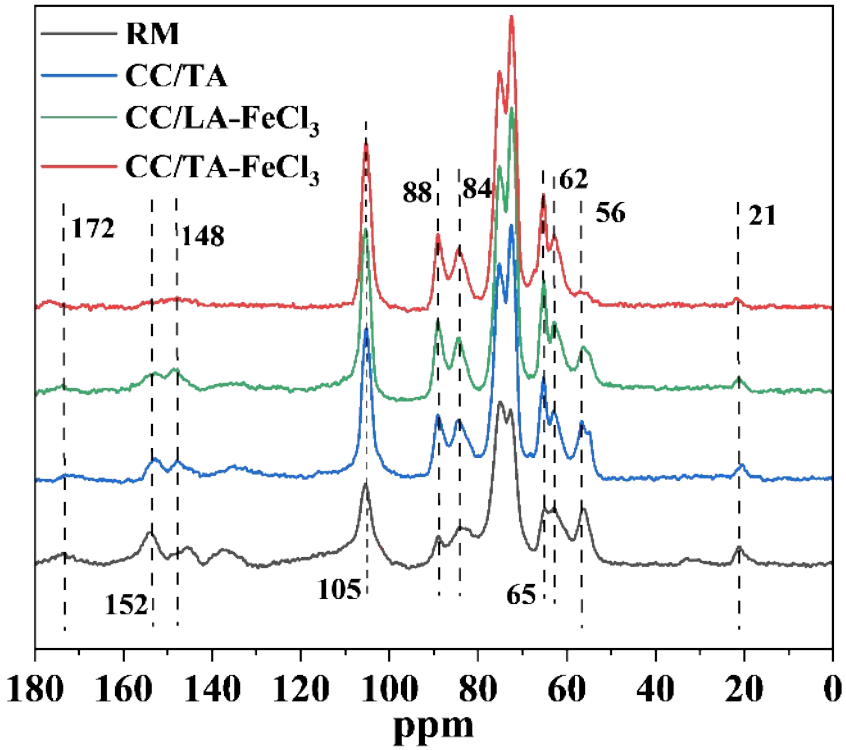

Fig. S4. CP/MAS ^{13}C NMR analysis of eucalyptus substrate before and after different DES treatment

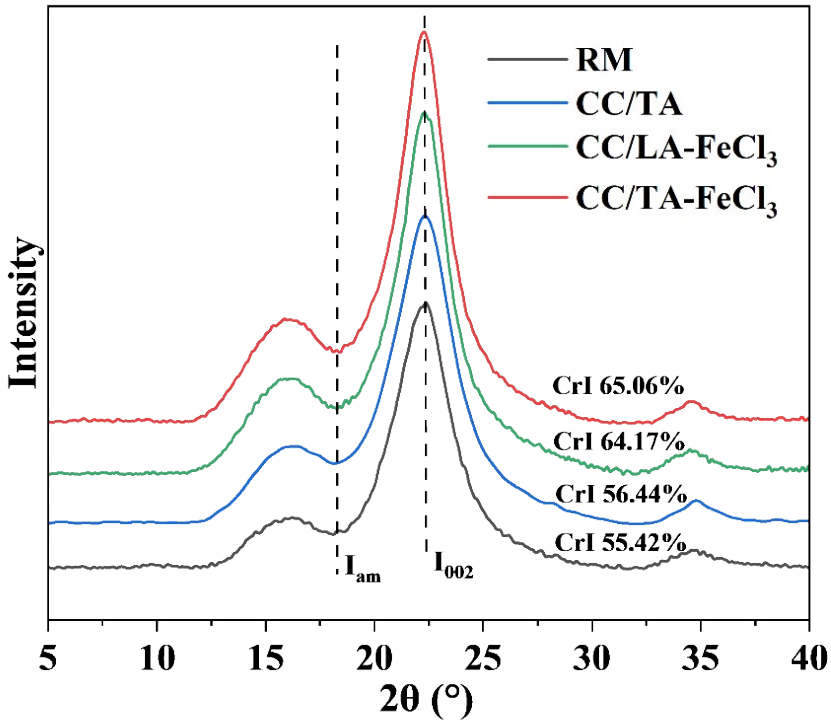

Fig. S5. XRD analysis of eucalyptus substrate before and after different DES treatment

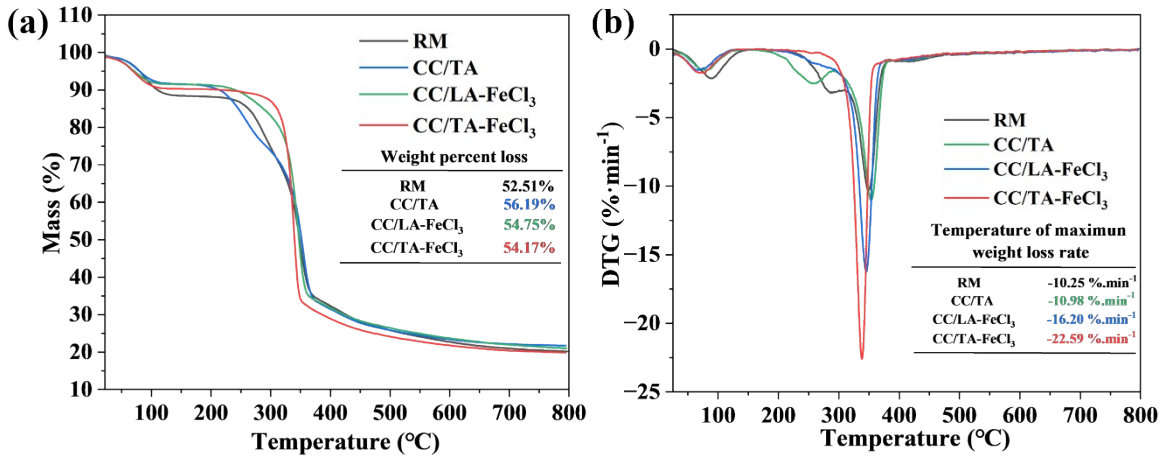

Fig. S6. TGA (a) and DTG (b) analysis of eucalyptus substrate before and after different DES treatment

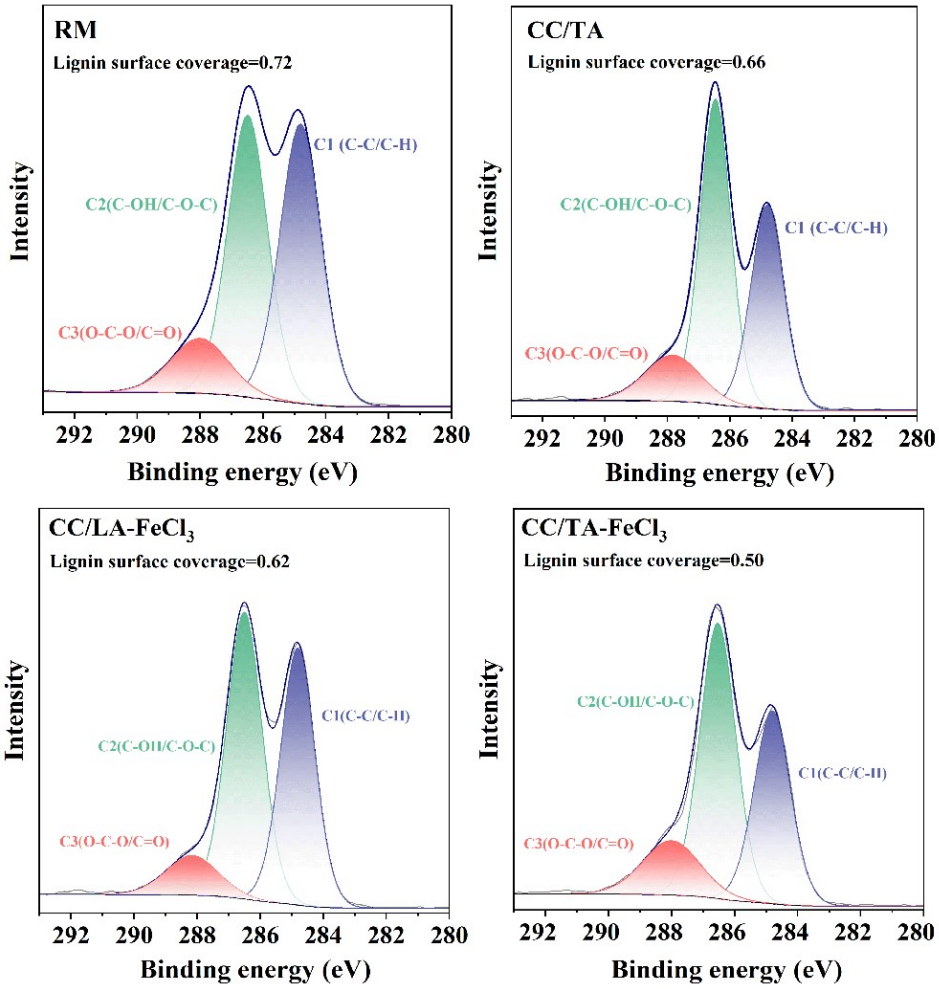

Fig. S7. XPS analysis of eucalyptus substrate before and after different DES treatment

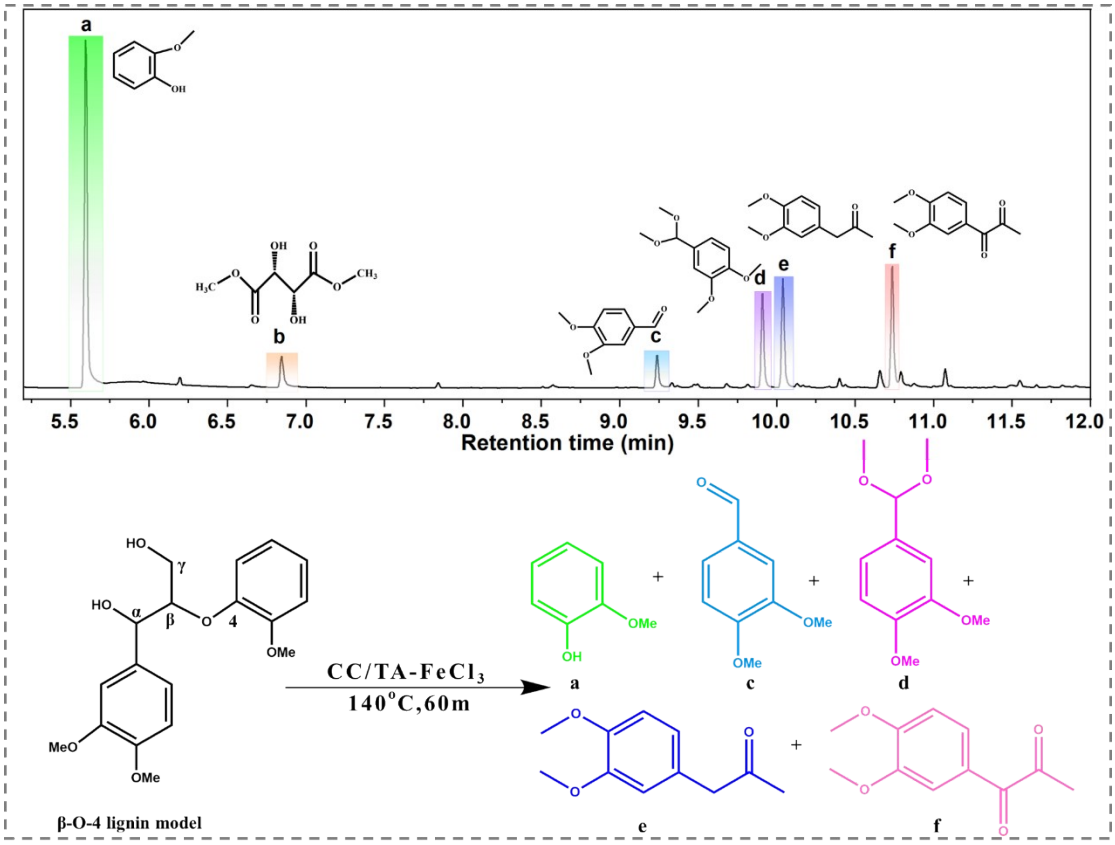

Fig. S8. Product analysis of β-O-4 Lignin Model Compounds using GC-MS

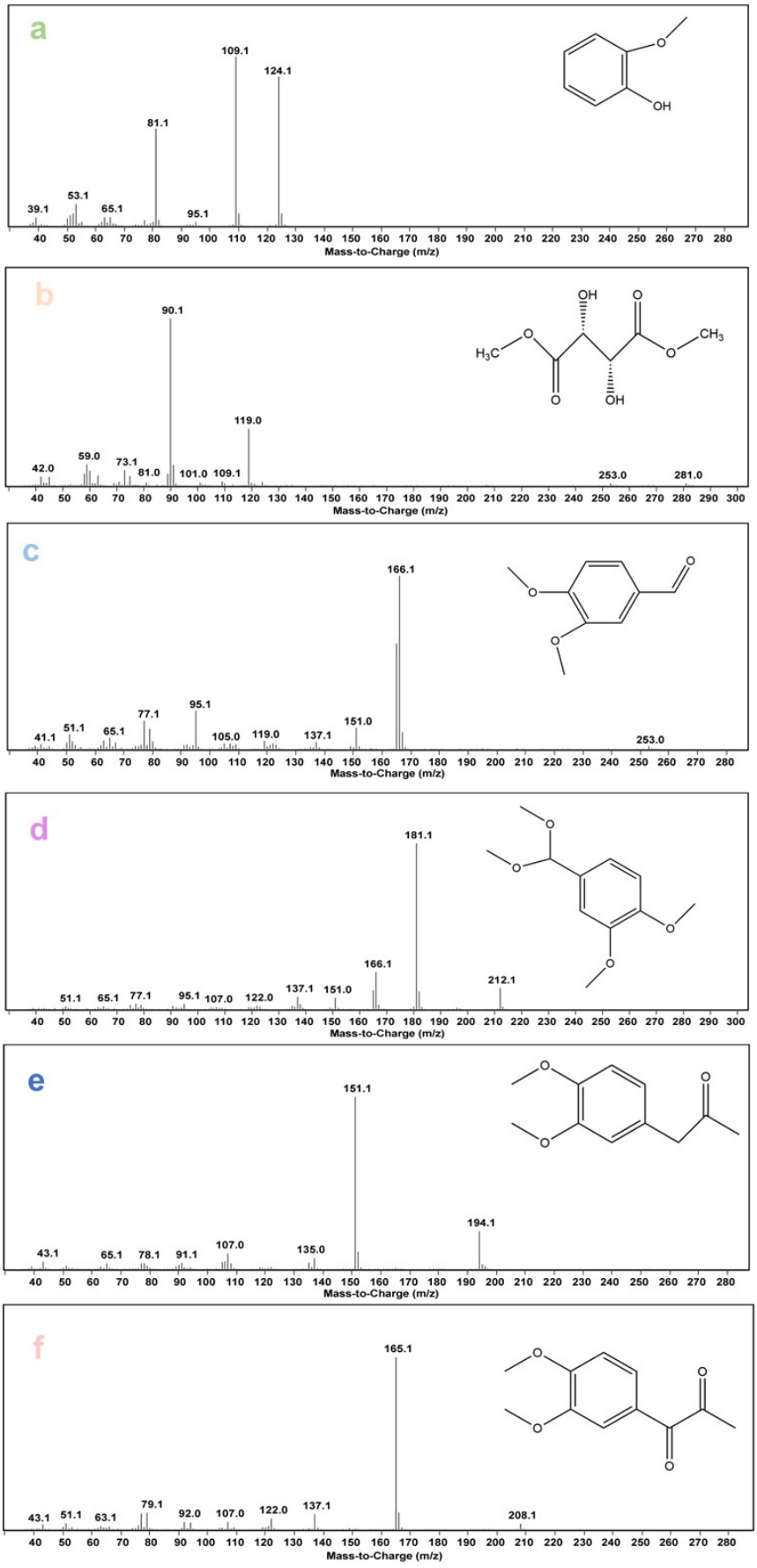

Fig. S9. Mass spectra of β-O-4 model compound after bond break

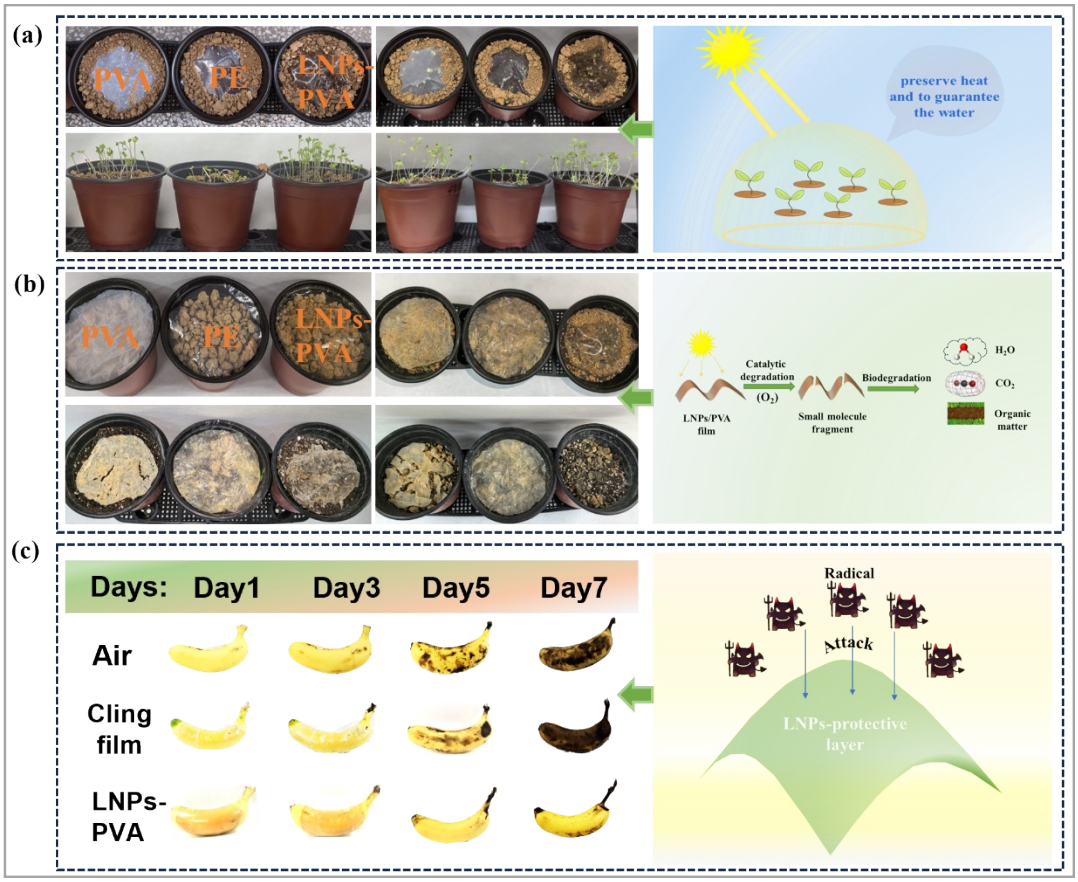

Fig. S10. Application evaluation of LNPs/PVA film. (a) Promote plant growth; (b) Microbial degradation; (c) Food preservation.

Table S1 Effects of different pretreatment methods on separation efficiency of main components of eucalyptus

Samples	Separation yield of cellulose (%)	Separation yield of hemicellulose (%)	Separation yield of lignin (%)
CC/TA treatment	6.32	34.25	13.02
CC/LA-$FeCl_3$ treatment	11.28	82.42	63.80
CC/TA-$FeCl_3$ treatment	10.35	73.03	71.93

Table S2 IC_{50} values of MWL and lignin isolated by different DESs pretreatments

Sample	MWL	CC/TA-L	CC/LA-$FeCl_3$-L	CC/TA-$FeCl_3$-L
IC_{50} (mg/mL)	0.166	0.129	0.095	0.086

Table S3 Signal attribution of characteristic peaks in 2D HSQC NMR spectra

Code	δC/δH (ppm)	Signal attribution
$-OCH_3$	55.7/3.75	C-H in methoxy
A_α	71.9/4.86	C-H in α position of β-O-4
A_β(S)	86.2/4.15	C-H in β position of β-O-4 (S)
A_β(G)	83.5/4.31	C-H in β position of β-O-4 (G)
A_γ	60.0/3.61	C-H in γ position of β-O-4
B_α	85.2/4.71	C-H in α position of resin alcohol
B_β	53.8/3.12	C-H in β position of resin alcohol
B_γ	71.4/3.81 and 4.18	C-H in γ position of resin alcohol
C_α	86.9/5.50	C-H in α position of phenyl coumarine
C_γ	62.5/3.74	C-H in γ position of phenyl coumarine
$S_{2,6}$	104.6/6.51	$C_{2,6}$-$H_{2,6}$ in S unit
$S'_{2,6}$	106.4/7.20	$C_{2,6}$-$H_{2,6}$ in oxidized S unit
G_2	111.5/6.99	C_2-H_2 in G unit
G_5	115.5/6.94	C_5-H_5 in G unit
G_6	118.7/6.81	C_6-H_6 in G unit

Table S4 Signal attribution of characteristic peaks in ^{31}P NMR spectra

Functional Group	Chemical shift (ppm)
Internal Standard	151.28-152.48
Aliphatic -OH	150.0-145.4
S-OH	144.0-142.4
G-OH	140.5-139.0
Phenolic -OH	144.0-137.8
-COOH	136.0-133.6